Coarsening kinetics of cuboidal γ' precipitates in single crystal nickel base superalloy CMSX-4

J. Lapin[1]*, M. Gebura[1], T. Pelachová[1], M. Nazmy[2]

[1] *Institute of Materials and Machine Mechanics, Slovak Academy of Sciences, Račianska 75, 831 02 Bratislava, Slovak Republic*
[2] *ALSTOM Ltd., Department of Materials Technology, TTTM, CH-5401 Baden, Switzerland*

Received 28 September 2008, received in revised form 3 November 2008, accepted 3 November 2008

Abstract

Coarsening kinetics of cuboidal γ' precipitates was studied in a single crystal nickel base superalloy CMSX-4 at five temperatures ranging from 850 to 1000 °C and five ageing times from 100 to 2000 h. The γ' precipitates preserve their cuboidal shape morphology during ageing at temperatures from 850 to 950 °C up to 2000 h. At a higher ageing temperature of 1000 °C, the cuboidal shape is preserved up to 500 h and longer ageing time leads to directional coarsening of the precipitates and formation of spontaneously rafted microstructure. The coarsening kinetics of cuboidal γ' precipitates follows cube rate law and is controlled by volume diffusion of alloying elements in the γ matrix according to Lifshitz-Slyozov-Wagner (LSW) theory. The activation energy for coarsening is calculated to be 272.4 kJ mol^{-1}. Critical input parameters such as γ/γ' interfacial energy and the effective diffusion coefficient controlling coarsening kinetics of the γ' precipitates are estimated and verified by comparing the calculated and experimental coarsening rate coefficients with those published for numerous multicomponent as well as binary nickel base alloys.

K e y w o r d s: nickel alloy, single crystal superalloy, ageing, coarsening kinetics, microstructure degradation

1. Introduction

Nickel base superalloys [1–6] are widely used in many applications as high-temperature structural materials because of their unusual ability to retain excellent combinations of mechanical properties and corrosion resistance at high temperatures comparing with other materials such as titanium base alloys [7–13], iron base alloys [14–16] or structural ceramics [17–20]. A typical microstructure of these superalloys usually contains $L1_2$-ordered γ' ($Ni_3(Al,Ti)$) precipitates coherently embedded in γ (Ni base solid solution) matrix with face-centered cubic crystal structure. The mechanical properties of nickel base superalloys depend on the volume fraction, distribution, size and morphology of γ' precipitates. With sufficient thermal energy, the γ' precipitates undergo coarsening. Since this may occur at later stages of the precipitation process or service at high temperatures, the coarsening of γ' precipitates represents a significant contribution to degradation processes affecting performance and service life of critical gas turbine components such as single crystal turbine blades. Hence, it is important to predict the coarsening kinetics of γ' precipitates at temperatures corresponding to those of turbine components.

The original theory of volume-diffusion controlled coarsening was developed by Lifshitz and Slyozov [21], Wagner [22] and recently reviewed by Baldan [23]. According to this theory, particle coarsening process involves competitive growth in which the larger particles grow at the expense of the small ones and the total number of precipitates in the system decreases. The driving force for such particle growth is the reduction in the total interfacial energy of the system. The rate of coarsening is governed by the rate at which solute is transferred through the matrix from the shrinking particles to the growing ones. However, Lifshitz-Slyozov-Wagner (LSW) theory was developed for sys-

*Corresponding author: tel.: +421 2 49268290; fax: +421 2 44253301; e-mail address: ummslapi@savba.sk

tems with small volume fraction of particles approaching zero. Obviously, this zero volume fraction approximation is not valid for nickel base superalloys where the precipitate volume fraction is often as high as 70 vol.%. As a result of the deficiencies in the LSW treatment, many theories of Ostwald coarsening of γ' particles based on multi-particle diffusion solution were developed [23–26]. However, they are all based on the same growth equation made by Lifshitz, Slyozov and Wagner [21, 22].

The aim of the present work is to study coarsening kinetics of γ' precipitates in single crystal superalloy CMSX-4. The alloy CMSX-4 is a cast nickel base superalloy, which is mainly used in manufacturing single crystal high-pressure turbine blades for aircraft engines and stationary gas turbines for power engineering.

2. Experimental procedure

The alloy CMSX-4 with the chemical composition Ni-7.0Cr-9.0Co-0.6Mo-6.0W-7.0Ta-3.0Re-5.6Al--1.0Ti-0.1Hf (wt.%) was provided by Cannon Muskegon (USA) in the form of a cylindrical ingot with a diameter of 60 mm and a length of 110 mm. The ingot was cut to smaller pieces using spark machining and lathe machined to cylindrical rods with a diameter of 8 mm and a length of 110 mm. Single crystal samples were prepared by seeding using seeds with [001] crystallographic orientation. Both the seed and cylindrical rod were put into a high-purity alumina mould (99.5 %) and directionally solidified (DS) in a modified Bridgman type apparatus described elsewhere [27]. All samples were directionally solidified at a constant growth rate of $V = 2.78 \times 10^{-5}$ m s^{-1} and constant temperature gradient in liquid at the solid-liquid interface of $G_L = 1 \times 10^4$ K m^{-1} under argon atmosphere (purity 99.995 %). Number of grains in each DS sample was verified metallographically using two transverse sections from the bottom and upper part of the sample. After directional solidification the single crystal samples were subjected to heat treatments consisting of solution annealing at 1315 ℃ for 6 h, quenching and two steps precipitation annealing at 1140 ℃ for 6 h and 870 ℃ for 20 h in argon. Ageing experiments were performed on samples with a diameter of 8 mm and thickness of 5 mm at five temperatures of 850, 900, 925, 950 and 1000 ℃ for different times ranging from 100 to 2000 h in air. Since the CMSX-4 superalloy exhibits an excellent high temperature oxidation resistance, no special surface protection was required up to an ageing temperature of 1000 ℃ [28].

Microstructural analysis was performed by light optical microscopy (OM) and scanning electron mi-

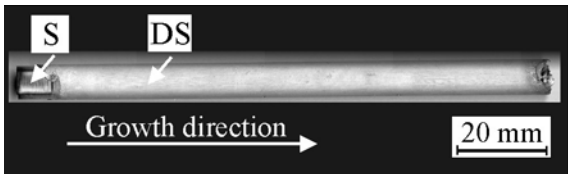

Fig. 1. Single crystal cylindrical sample after directional solidification at $V = 2.78 \times 10^{-5}$ m s^{-1} and $G_L = 1 \times 10^4$ K m^{-1}: S – unmelted part of the seed, DS – directionally solidified part of the sample.

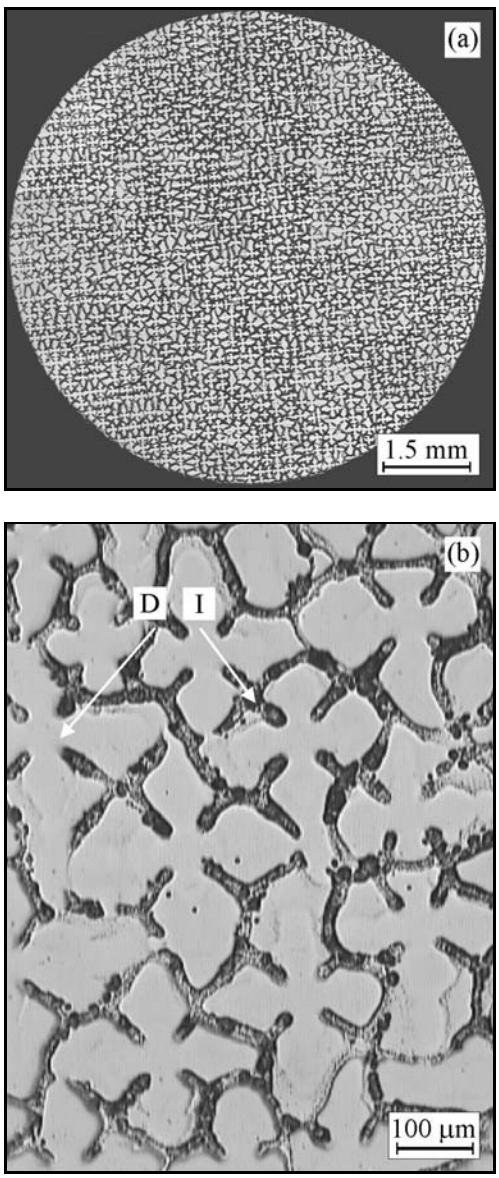

Fig. 2. OM micrograph showing the typical microstructure on transverse section of cylindrical samples after directional solidification at $V = 2.78 \times 10^{-5}$ m s^{-1} and $G_L = 1 \times 10^4$ K m^{-1}: (a) distribution of dendrites in single crystal sample, (b) detail of dendritic microstructure. D – dendrite, I – interdendritic region.

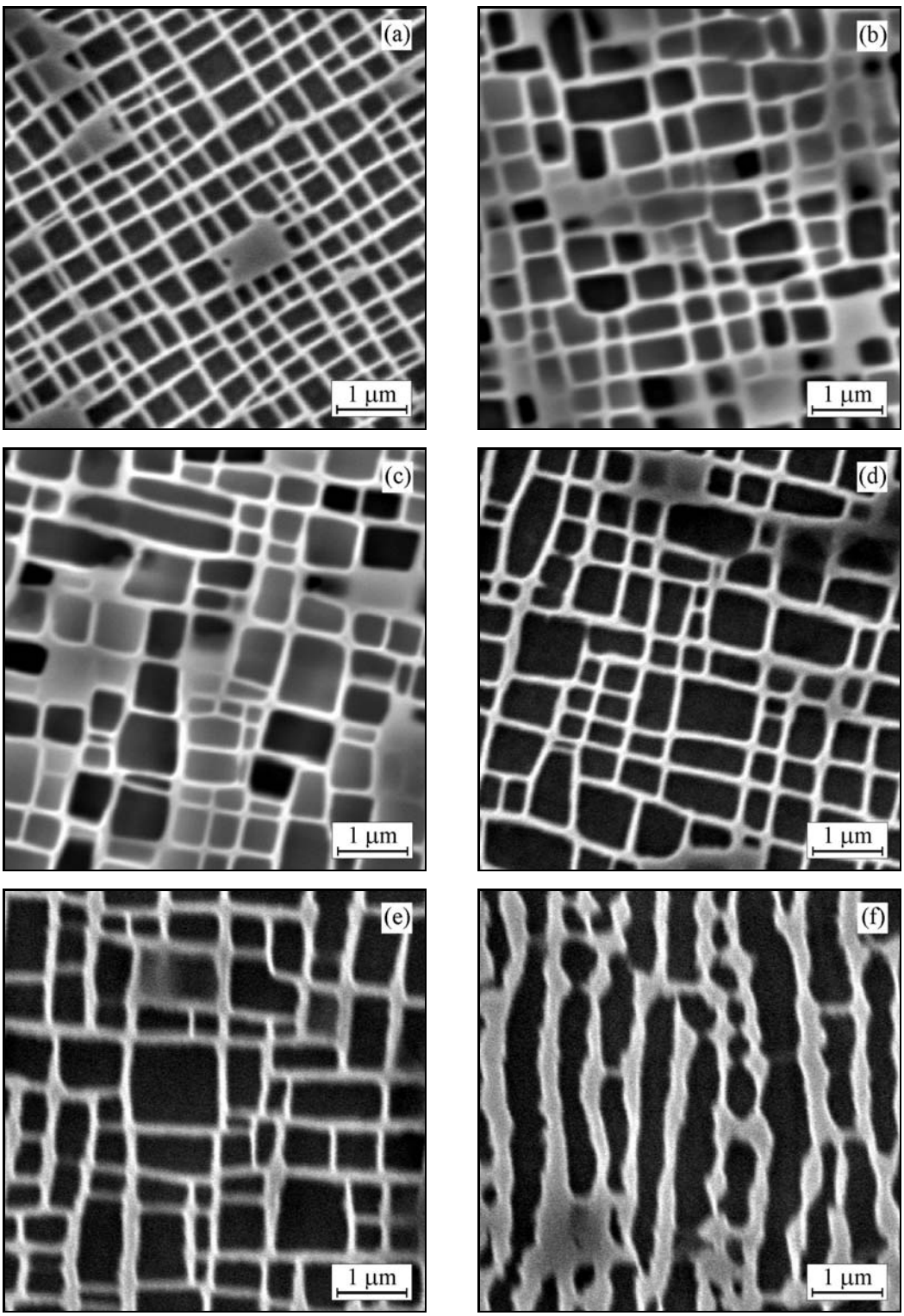

Fig. 3. SEM micrographs showing the effect of ageing on morphology of cuboidal γ' precipitates: (a) initial microstructure before ageing, (b) ageing at 950 °C for 500 h, (c) ageing at 950 °C for 1000 h, (d) ageing at 950 °C for 2000 h, (e) ageing at 1000 °C for 500 h, (f) ageing at 1000 °C for 1000 h.

croscopy (SEM). OM and SEM samples were prepared using standard metallographic techniques and etched in a reagent of 12.5 ml alcohol, 12.5 ml HNO_3 and 13.5 ml HCl. Size and volume fraction of γ' precipitates were measured on digitalized micrographs using a computerized image analyser.

3. Results

3.1. Microstructure after directional solidification and heat treatments

Figure 1 shows a sample after directional solidification in the [001] crystallographic direction. It is clear that the seed (S) was melted only partially and there is an excellent junction between the seed and the remaining part of DS sample. Figure 2 shows the typical microstructure on a transverse section of DS samples after directional solidification. The sample was a single crystal with well-oriented dendrites, as illustrated in Fig. 2a. The dendrites are light-grey coloured and the interdendritic region is dark-grey, as seen in Fig. 2b. The average primary dendrite arm spacing was measured to be 230 μm. Figure 3 shows morphology of γ' precipitates after heat treatments and ageing. Figure 3a shows initial microstructure of the alloy before ageing. Nearly square sections of the γ' precipitates on (001) crystallographic plane as well as similar nearly square sections on (010) and (100) crystallographic planes confirmed their cuboidal morphology before ageing. Volume fraction of the γ' precipitates was measured to be (69 ± 1) vol.% and remained constant within the experimental error of measurements during ageing.

3.2. Effect of ageing on morphology and size of γ' precipitates

Figures 3b to 3d show the effect of ageing at 950 °C on morphology of the γ' precipitates. It is clear that a nearly square section, which is the typical shape on {001} crystallographic planes, confirms that cuboidal morphology of the precipitates is preserved during ageing up to 2000 h. On the other hand, higher ageing temperature of 1000 °C and longer ageing time than 500 h (Fig. 3e) results in transformation of cuboidal precipitates to elongated ones, as shown in Fig. 3f. As shown recently by Gebura and Lapin [29], formation of elongated γ' precipitates is connected with development of spontaneous rafted microstructure, which is formed initially within the dendrites and then in the interdendritic region during isothermal ageing of the CMSX-4 superalloy for long ageing time. In order to avoid the effect of morphological changes on coarsening kinetics of cuboidal γ' precipitates, morphological stability of the γ' precipitates was evaluated from their shape factor F defined as

$$F = \frac{4\pi A}{P^2} \,, \tag{1}$$

where A and P is the cross sectional area and perimeter of the γ' precipitate on {001} crystallographic planes, respectively. Taking into account Eq. (1), one can calculate a shape factor of 1 and 0.785 for a circle and an ideal square, respectively. Figure 4 shows evolution of shape factor of the γ' precipitates with the ageing time at five applied ageing temperatures. The shape factor ranges from 0.749 to 0.788 and is very close to a theoretical value of 0.785 representing an ideal square. The measured values of the shape factor indicate stability of the cuboidal γ' precipitates during ageing at temperatures ranging from 850 to 950 °C for up to 2000 h. On the other hand, the ageing at 1000 °C is connected with a sudden drop of the shape factor from 0.79 measured after ageing for 500 h to a value of 0.24 after 1000 h, which is connected with a development of spontaneously rafted microstructure in the alloy [29].

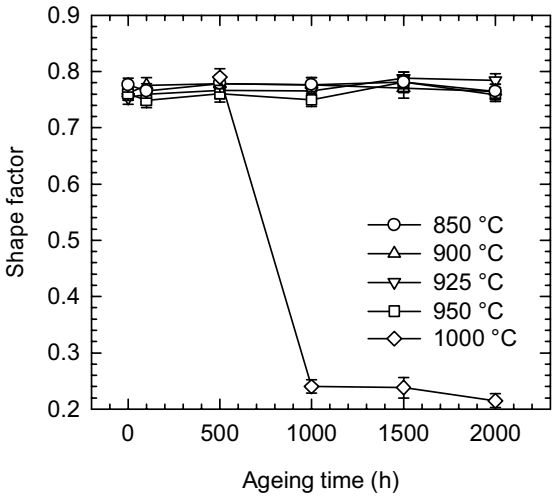

Fig. 4. Dependence of shape factor of the γ' precipitates on ageing time. The ageing temperatures are indicated in the figure.

3.3. Coarsening kinetics of cuboidal γ' precipitates

The measured statistical data (minimum 1000 precipitates measured at each ageing regime) of size defined as an edge length a_m of the cuboidal γ' precipitates were fitted by a log-normal distribution function $\varphi(a_\mathrm{m})$ in the form

$$\varphi\left(a_\mathrm{m}\right) = \frac{1}{\sigma_\mathrm{s}\sqrt{2\pi}} \exp\left[-\frac{\left(\ln a_\mathrm{m} - \ln a\right)^2}{2\sigma_\mathrm{s}^2}\right], \tag{2}$$

where a is the mean value and σ_s is the variance of log-normal distribution. Figure 5 shows log-normal distribution curves resulting from the statistical evaluation of the size of γ' precipitates after ageing at 950 °C. Figure 6 shows dependence of mean size of γ' precipitates on the ageing time. The mean size a increases with

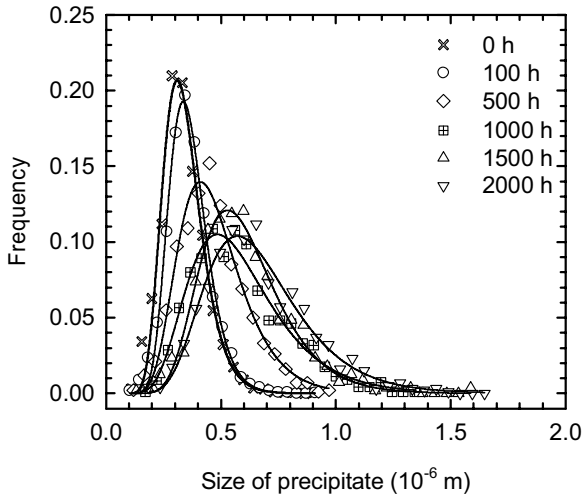

Fig. 5. Examples of log-normal distribution curves for size of cuboidal γ' precipitates after ageing at 950 °C. The ageing times are indicated in the figure.

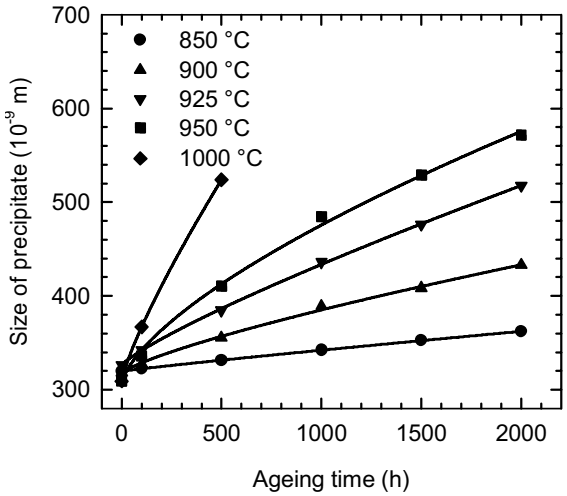

Fig. 6. Dependence of mean size of the γ' precipitates on ageing time. The ageing temperatures are indicated in the figure.

increasing ageing time and temperature. The LSW theory predicts that the mean size of precipitates a increases with time t according to the following equation [23]

$$a^3 - a_0^3 = kt, \tag{3}$$

where a_0 is the mean size of γ' precipitates at ageing time $t = 0$ s and k is a material constant at a given temperature. Figure 7 shows dependence of normalized size of γ' precipitates on the ageing time. It is clear that the normalized size values can be well fitted by a linear regression function according to Eq. (3) at each studied temperature. The correlation coefficients r^2 of these fits are better than 0.98.

Assuming material constants k obtained from linear regression analysis of experimental data shown in Fig. 7, the activation energy for coarsening of cuboidal γ' precipitates can be calculated according to equation in the form

$$k = k_0 \exp\left(-\frac{Q}{RT}\right), \tag{4}$$

where k_0 is a material constant, Q is the activation energy for coarsening, R is the universal gas constant and T is the absolute temperature. Figure 8 shows dependence of material constant k on inverse temperature in the form of Arrhenius diagram. From this figure, the activation energy for coarsening is calculated to be $272.4 \pm 2.3\,\mathrm{kJ\,mol^{-1}}$. This activation energy for coarsening of cuboidal γ' precipitates can be compared with values ranging from 247 to $280\,\mathrm{kJ\,mol^{-1}}$, which were reported for various nickel base alloys, as summarized in Table 1 [30–37]. It is clear that the measured $Q = 272.4\,\mathrm{kJ\,mol^{-1}}$ corresponds very well to a value of $272\,\mathrm{kJ\ mol^{-1}}$ reported by Kim et al. [35] for Ni-10.4Cr-8.W-1.8Mo-4.4Al-1Ti-1.1Nb-8.3Co--3.2Ta-0.8Hf-0.1Zr-0.02B-0.1C (wt.%) alloy and is very close to values of $268\,\mathrm{kJ\,mol^{-1}}$ and $277\,\mathrm{kJ\,mol^{-1}}$ reported for Ni-14Mo-6.2Al-6.2Ta (wt.%) and Ni-8.5Cr-9.7W-1.8Mo-4.5Al-1Ti-1Nb-9.6Co-5.2Ta--0.1Hf-0.1Zr-0.01B-0.1C (wt.%) alloys, respectively [30, 35]. Figure 9 shows dependence of mean size of the precipitates $a^3 - a_0^3$ normalized by the activation energy for coarsening Q, absolute temperature and universal gas constant on the ageing time. Using linear regression analysis, the kinetic equation for coarsen-

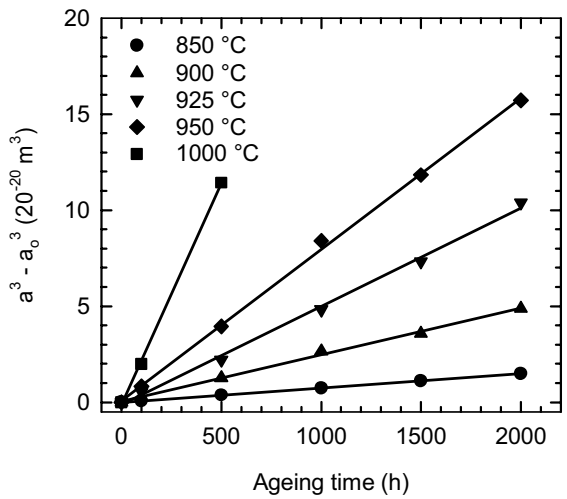

Fig. 7. Dependence of normalized size of the γ' precipitates on ageing time. The ageing temperatures are indicated in the figure.

Table 1. Activation energy for coarsening of γ' precipitates Q in various nickel base alloys

Alloy composition (wt.%)	Activation energy for coarsening Q (kJ mol^{-1})	Ageing temperature (°C)	Ageing time (h)	Reference
Ni-14Mo-6.2Al-6.2Ta	268	927–1093	0–100	[30]
Ni-24.3Cr-19.6Co-1.8Nb-1.6Ti-0.75Al0.52Mo-1.02Fe--0.3Mn-0.5Si-0.03C	247	704–760	0–4000	[31]
Ni-1Ti-5.62Al-6Ta-7.9W-0.6Mo-4.6Co-7.8Cr (CMSX-2)	256–263	800–950	0–1000	[32]
Ni-15.5Cr-10.8Co-5.6W-2.1Mo-3.2Al-4.6Ti-0.2Nb-0.4Hf--0.08B-0.07C	255	800–900	0–10000	[33]
Ni-33.8Fe-16.5Cr-1.24Al-1.2Ti-0.27Co-3.3Mo-0.26Si (Nimonic PE 16)	280	700–850	0–1000	[34]
Ni-10.4Cr-8.W-1.8Mo-4.4Al-1Ti-1.1Nb-8.3Co-3.2Ta--0.8Hf-0.1Zr-0.02B-0.1C	272	870–1020	0–300	[35]
Ni-8.5Cr-9.7W-1.8Mo-4.5Al-1Ti-1Nb-9.6Co-5.2Ta--0.1Hf-0.1Zr-0.01B-0.1C	277	870–1020	0–300	[35]
Ni-6.8Al-12Mo-7.6Ta	255	800–1100	0–100	[36]
Ni-6.8Al-12Mo-7.7W	251	800–1100	0–100	[36]
Ni-6.2Al	262.5	550–700	0–200	[37]
Ni-7Cr-9Co-0.6Mo-6W-7Ta-5.6Al-1Ti-0.1Hf-3Re (CMSX-4)	272.4	850–1000	0–2000	Present work

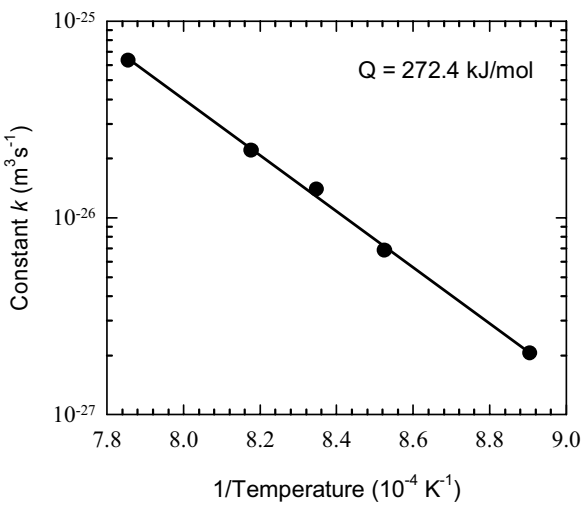

Fig. 8. Arrhenius diagram showing the dependence of the material constant k on the inverse temperature.

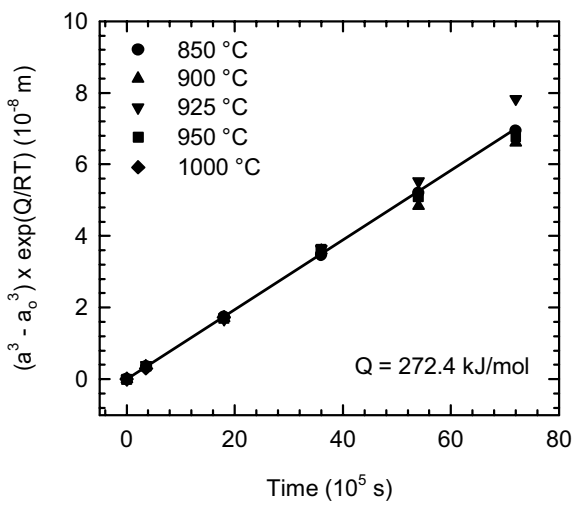

Fig. 9. Dependence of mean size of precipitates $a^3 - a_0^3$ normalized by the activation energy for coarsening Q, absolute temperature and universal gas constant on the ageing time.

ing of cuboidal γ' precipitates can be written in the form

$$a^3 - a_0^3 = 9.724 \times 10^{-15} t \exp\left(-\frac{272400}{RT}\right) . \quad (5)$$

The correlation coefficient r^2 of this fit is 0.98.

4. Discussion

The experimental coarsening data show a cube rate law which suggests that volume diffusion controls coarsening process of the γ' precipitates in the studied CMSX-4 superalloy as long as the particles remain discrete and cuboidal. It is worth to analyse whether the coarsening kinetics of the γ' precipitates can be predicted analytically using physically sound thermodynamic data according to a standard LSW coarsening equation in the form [23]

$$\left(a^3 - a_0^3\right)^{1/3} = k_1 t^{1/3}, \quad (6)$$

where k_1 is the coarsening rate coefficient defined as

$$k_1 = \left(\frac{64 D_{\text{eff}} C_\infty \sigma \Omega^2}{9RT} \right)^{1/3}, \quad (7)$$

where C_∞ is the molar solid solubility of controlling solute in the matrix, σ is the precipitate/matrix interfacial energy, Ω is the molar volume of the precipitate and D_{eff} is the effective diffusion coefficient. The effective diffusion coefficient in the γ matrix should be related to the fluxes of all n components according to relationship in the form [38]

$$D_{\text{eff}} = D_{\text{o}} \exp\left(-\frac{Q_{\text{eff}}}{RT} \right), \quad (8)$$

where the pre-exponential factor D_{o} is defined as

$$D_{\text{o}} = \sum_{i=1}^{n} x_i D_{\text{o}i}, \quad (9)$$

where x_i is the mole fraction of i-th element in the γ' precipitate and $D_{\text{o}i}$ is the pre-exponential factor of i-th element in the γ matrix. The effective activation energy for diffusion Q_{eff} is defined as

$$Q_{\text{eff}} = \sum_{i=1}^{n} x_i Q_i, \quad (10)$$

where Q_i is the activation energy for volume diffusion of i-th element in the γ matrix.

Assuming Eq. (7), at minimum one critical input parameter has to be calculated by fitting experimental data. The attempt will be made to derive either effective diffusion coefficient D_{eff} or interfacial energy between the γ matrix and γ' precipitate σ, which are both unclear input data for the studied CMSX-4 superalloy.

Firstly, an effective diffusion coefficient will be derived to fit experimental coarsening data for the studied CMSX-4 superalloy. As results from the chemical composition of the γ' precipitates of Ni-8.6Al--1.4Ti-8.7Ta-2Cr-5.8Co-5.7W-0.7Mo-0.6Re (wt.%) and the γ matrix of Ni-0.8Al-0.2Ti-0.6Ta-16.5Cr--17.4Co-8.2W-1.6Mo-9.2Re (wt.%) reported by Wanderka and Glatzel [39], the main element which should be transferred from a dissolving γ' precipitate to a growing one is Al and in less extent Ti, Ta and other elements. Since no reliable data are available for diffusion coefficients of the alloying elements in the γ matrix of CMSX-4 superalloy, we can only refer to values calculated according to Eq. (8) and taking data of $Q_{\text{eff}} = 272\,\text{kJ mol}^{-1}$ and $D_{\text{o}} = 3.9 \times 10^{-5}\,\text{m}^2\,\text{s}^{-1}$ measured for volume diffusion of Al in ternary Ni-Al-Ti alloy by Karunaratne et al. [40]. Due to very good agreement between the effective activation energy for volume diffusion Q_{eff} and activation energy for coarsening of the cuboidal γ' precipitates, only the pre-exponential factor D_{o} will be used as a fitting parameter. Since there is lack of available literature data about the solid solubility of Al in the γ matrix of the studied CMSX-4 superalloy, the values of 6.55, 6.90, 7.17, 7.48, and 8.57 (at.%) measured for nickel base superalloy Udimet 700 with the chemical composition given in Table 2 at 850, 900, 925, 950, and 1000 °C, respectively, will be used in our calculations [41]. The corresponding calculated molar solubility C_∞ of Al in the γ matrix (density of the matrix is assumed to be $8700\,\text{kg m}^{-3}$) is 9093, 9609, 9996, 10447 and $12027\,\text{mol m}^{-3}$ at 850, 900, 925, 950 and 1000 °C, respectively. For the γ' precipitate/γ matrix interfacial energy σ, we can refer to values ranging from 6 to $90\,\text{mJ m}^{-2}$ [42–45]. The value of σ depends on a large number of factors such as temperature, composition of the γ matrix, and volume fraction of γ' precipitates. Since no data are available about the temperature dependence of interfacial energy σ for the superalloy CMSX-4, the values of Li et al. [38] calculated for superalloy Nimonic 115 with the chemical composition given in Table 2 were used in the form of $\sigma = 94.603–0.0368\ T$, where temperature T is in °C and σ is in mJ m^{-2}. Assuming Eq. (7) and taking reduced pre-exponential factor of $D_{\text{o}} = 2.7 \times 10^{-5}\,\text{m}^2\,\text{s}^{-1}$, one can calculate coarsening rate coefficient k_1 for the cuboidal γ' precipitates in CMSX-4 alloy at each ageing temperature. Figure 10 shows temperature dependence of calculated and experimentally measured coarsening rate exponents for the γ' precipitates in the studied CMSX-4. It is clear

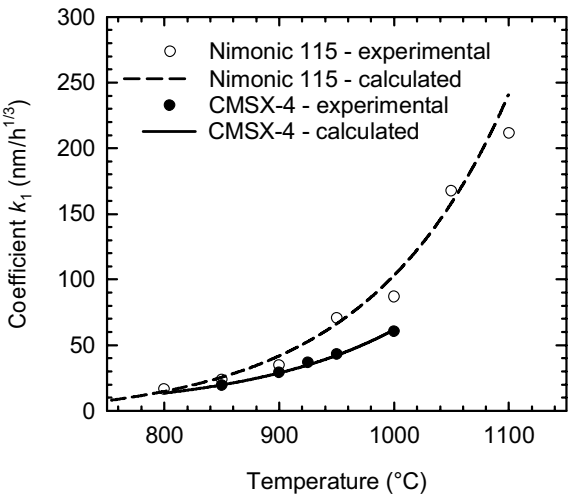

Fig. 10. Comparison between calculated and experimentally measured coarsening rate coefficient k_1 in the studied CMSX-4 and Nimonic 115 [38] superalloys as a function of temperature.

Table 2. Chemical composition (in wt.%) of multicomponent Ni base alloys shown in Fig. 11

Alloy	Ni	Al	Cr	Co	W	Ta	Ti	Mo	Other
Nimonic 80A	Bal.	1.4	19.5				2.4		
Nimonic 90	Bal.	1.5	19.5	16.5			2.5		
Nimonic 105	Bal.	4.7	15.0	20.0			1.3	5.0	
Nimonic 115	Bal.	4.9	14.2	13.2			3.8	3.2	
Nimonic 263	Bal.	0.5	20.0	20.0			2.9	5.8	
PE 11	Bal.	0.8	18.0				2.3	5.2	34 Fe
PE 16	Bal.	1.2	16.5				1.2	3.3	34 Fe
PK 33	Bal.	2.1	18.0	14.0			2.4	7.0	
Udimet 700	Bal.	4.5	15.0	19.0			3.5	5.0	4 Fe
IN-738	Bal.	3.4	16.0	8.5	2.6	1.7	3.4	1.7	0.9 Nb
CMSX-4	Bal.	5.6	7.0	9.0	6.0	7.0	1.0	0.6	0.1 Hf-3Re

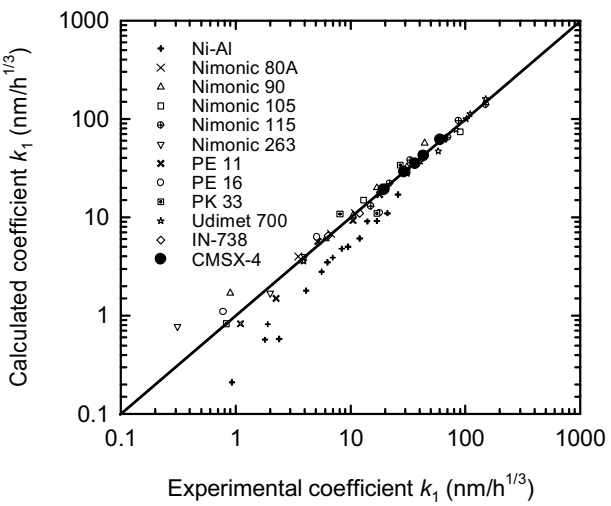

Fig. 11. Dependence of calculated coarsening rate coefficient k_1 on experimentally determined one for the studied CMSX-4 superalloy and various nickel base alloys reported by Li et al. [38]. The chemical composition of multicomponent nickel base alloys is given in Table 2.

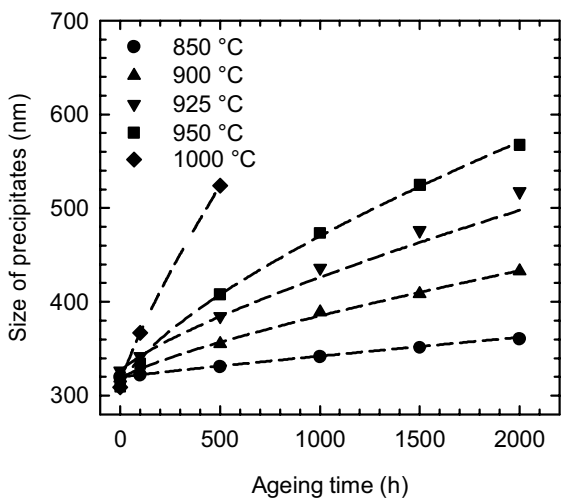

Fig. 12. Dependence of experimentally measured (full points) and calculated (dashed lines) size of the γ' precipitates as a function of ageing time. The ageing temperatures are indicated in the figure.

that the CMSX-4 shows significantly lower coarsening rate coefficients than those of Nimonic 115 [38] over the studied temperature range. As a validation of this approach, coarsening rate coefficients k_1 of the studied CMSX-4 are compared with those of numerous multicomponent nickel base alloys as well as with binary Ni-Al systems reported by Li et al. [38]. Figure 11 shows summary graph of dependence of calculated coarsening rate coefficient k_1 on experimentally determined one. It is clear that the results for the CMSX-4 are in a very good agreement with those for multicomponent alloys with the chemical composition given in Table 2 but deviates from the results for binary Ni-Al alloys, where the coarsening rate coefficients were calculated by Li et al. [38] to be too slow.

Secondly, temperature dependence values of γ' precipitate/γ matrix interfacial energy σ will be derived to fit experimental coarsening data for the studied CMSX-4 superalloy. Assuming Eq. (7) and taking $Q_{\text{eff}} = 272\,\text{kJ mol}^{-1}$, $D_{\text{o}} = 3.9 \times 10^{-5}$ m^2 s^{-1} [40] and the same values of molar solubility C_∞ [41] of Al in the γ matrix as in the previous calculations, the same coarsening rate coefficients k_1 can be calculated using the values of γ' precipitate/γ matrix interfacial energy defined by a relationship in the form of $\sigma = 65.495 - 0.0254\,T$, where temperature T is in ℃ and σ is in mJ m^{-2}. Assuming ageing temperature range from 850 to 1000 ℃, the calculated interfacial energy values σ vary from 43.905 to 40.095 mJ m^{-2}.

Figure 12 shows evolution of experimentally measured and calculated size of the γ' precipitates with ageing time. The evolution of the size calculated either by using an effective diffusion coefficient or estimated values of γ/γ' interface energy corresponds very well

to the measured data and confirms the validity of the adjusted input parameters for calculations of mean size of the cuboidal γ' precipitates.

5. Conclusions

The investigation of coarsening kinetics of cuboidal γ' precipitates in single crystal nickel base superalloy CMSX-4 suggests the following conclusions:

1. During ageing at temperatures ranging from 850 to 950 °C up to 2000 h the γ' precipitates preserve their cuboidal shape. At a higher ageing temperature of 1000 °C the cuboidal shape of the precipitates is preserved up to 500 h and longer ageing time leads to their morphological instability characterized by directional coarsening and formation of spontaneously rafted microstructure.

2. The coarsening kinetics of cuboidal γ' follows a cube rate law behaviour and is controlled by volume diffusion of alloying elements in the γ matrix according to LSW theory. The calculated activation energy for coarsening of 272.4 kJ mol^{-1} corresponds to the activation energy for volume diffusion of Al in ternary Ni-Al-Ti alloys.

3. The coarsening rate coefficients of cuboidal γ' precipitates have been calculated by the method based on the LSW theory. Critical input parameters such as γ/γ' interfacial energy and the effective diffusion coefficient controlling coarsening kinetics of cuboidal γ' precipitates are estimated and verified by comparing the calculated and experimental coarsening rate coefficients with those published for numerous multicomponent as well as binary nickel base alloys.

Acknowledgements

This work was financially supported by the Slovak Grant Agency for Science under the contract VEGA 2/7085/27. The authors would like to express their gratitude to Dr. K. Harris from Cannon Muskegon Corporation (USA) for providing the ingot of CMSX-4 superalloy.

References

[1] SERIN, K.—GÖBENLI, G.—EGGELER, G.: Mater. Sci. Eng. A, *387–389*, 2004, p. 133.
[2] LUKÁŠ, P.—KUNZ, L.—SVOBODA, M.: Int. J. Fatigue, *27*, 2005, p. 1535.
[3] HAKL, J.—VLASÁK, T.—LAPIN, J.: Kovove Mater., *45*, 2007, p. 177.
[4] LAPIN, J.—MAREČEK, J.—KURSA, M.: Kovove Mater., *44*, 2006, p. 1.
[5] KUNZ, L.—LUKÁŠ, P.—MINTÁCH, R.—HRBÁČEK, K.: Kovove Mater., *44*, 2006, p. 275.
[6] CVIJOVIĆ, I.—SPIEGEL, M.—PAREZANOVIĆ, I.: Kovove Mater., *44*, 2006, p. 35.
[7] KUDRMAN, J.—FOUSEK, J.—BŘEZINA, V.—MÍKOVÁ, R.—VESELÝ, J.: Kovove Mater., *45*, 2007, p. 199.
[8] SANIN, V.—YUKHVID, V.—SYTSCHEV, A.—ANDREEV, D.: Kovove Mater., *44*, 2006, p. 49.
[9] LAPIN, J.—GABALCOVÁ, Z.—BAJANA, O.—DALOZ, D.: Kovove Mater., *44*, 2006, p. 297.
[10] LAPIN, J.: Kovove Mater., *44*, 2006, p. 57.
[11] GABALCOVÁ, Z.—LAPIN, J.: Kovove Mater., *45*, 2007, p. 231.
[12] LAPIN, J.—PELACHOVÁ, T.—DOMÁNKOVÁ, M.—DALOZ, D.—NAZMY, M.: Kovove Mater., *45*, 2007, p. 121.
[13] MOSKALEWICZ, T.—ZIMOWSKI, S.—KITANO, Y.—WIERZCHON, T.—CZYRSKA-FILEMONOWICZ, A.: Kovove Mater., *44*, 2006, p. 133.
[14] KRATOCHVÍL, P.—MÁLEK, P.—PEŠIČKA, J.—HAKL, J.—VLASÁK, T.—HANUS, P.: Kovove Mater., *44*, 2006, p. 185.
[15] KRATOCHVÍL, P.—SCHINDLER, I.—HANUS, P.: Kovove Mater., *44*, 2006, p. 321.
[16] VODIČKOVÁ, V.—KRATOCHVÍL, P.—DOBEŠ, F.: Kovove Mater., *45*, 2007, p. 153.
[17] DUSZA, J.—HVIZDOŠ, P.: Kovove Mater., *44*, 2006, p. 251.
[18] GONDÁR, E.—GÁBRIŠOVÁ, Z.—ROŠKO, M.—ZEMÁNKOVÁ, M.: Kovove Mater., *44*, 2006, p. 113.
[19] VYSOCKÁ, A.—ŠPAKOVÁ, J.—DUSZA, J.—BALOG, M.—ŠAJGALÍK, P.: Kovove Mater., *45*, 2007, p. 223.
[20] ŠPAKOVÁ, J.—VYSOCKÁ, A.—KOVALČÍK, J.—DUSZA, J.—LENKEY, G. B.: Kovove Mater., *45*, 2007, p. 209.
[21] LIFSHITZ, I. M.—SLYOZOV, V. V.: J. Phys. Chem. Solids, *19*, 1961, p. 35.
[22] WAGNER, C.: Z. Elektrochem., *65*, 1961, p. 581.
[23] BALDAN, A.: J. Mater. Sci., *37*, 2002, p. 2379.
[24] BRAILSFORD, A. D.—WYNBLATT, P.: J. Mater. Sci., *27*, 1979, p. 489.
[25] DAVIES, C. K. L.—NASH, P.—STEVENS, R. N.: Acta Metall., *28*, 1980, p. 179.
[26] VOORHEES, P. W.—GLICKSMAN, M. E.: Acta Metall., *32*, 1984, p. 2001.
[27] LAPIN, J.—ONDRÚŠ, Ľ.—NAZMY, M.: Intermetallics, *10*, 2002, p. 1019.
[28] LAPIN, J.—PELACHOVÁ, T.—MAREČEK, J.: In: 8th Liège Conference on Materials for Advanced Power Engineering. Eds.: Lecomte-Beckers, J., Carton, M., Schubert, F., Ennis, P. J. Jülich, Forschungszentrum Jülich GmbH 2006, vol. 53, part II, p. 803.
[29] GEBURA, M.—LAPIN, J.: In: 17th International Conference on Metallurgy and Materials Metal 2008. Ed.: Tanger, s. r. o., Ostrava 2008, CD ROM.
[30] MACKAY, R. A.—NATHAL, M. V.: Acta Metall. Mater., *38*, 1990, p. 993.
[31] SHUANGQUN, Z.—XISHAN, X.—GAYLORD, D. S.—SHAILESH, J. P.: Mater. Lett., *58*, 2004, p. 1784.
[32] GES, A. M.—FORNARO, O.—PALACIO, H. A.: Mater. Sci. Eng. A, *458*, 2007, p. 96.
[33] HOU, J. S.—GUO, J. T.: J. Mater. Eng. Perform., *15*, 2006, p. 67.

[34] BHANU SANKARA RAO, K.—SEETHARAMAN, V.—MANNAN, S. L.—RODRIGUEZ, P.: Mater. Sci. Eng., *58*, 1983, p. 93.
[35] KIM, H. T.—CHUN, S. S.—YAO, X. X.—FANG, Y.—CHOI, J.: J. Mater. Sci., *32*, 1997, p. 4917.
[36] SADIQ, S.—WEST, D. R. F.: Scripta Met., *19*, 1985, p. 833.
[37] MARSH, C.—HAYDN CHEN: Acta Metall. Mater., *38*, 1990, p. 2287.
[38] LI, X.—SAUNDERS, N.—MIODOWNIK, A. P.: Metall. Mater. Trans. A, *33A*, 2002, p. 3367.
[39] WANDERKA, N.—GLATZEL, U.: Mater. Sci. Eng. A, *203*, 1995, p. 69.
[40] KARUNARATNE, M. S. A.—CARTER, P.—REED, R. C.: Acta Mater., *49*, 2001, p. 861.
[41] VAN DER MOLEN, E. H.—OBLAK, J. M.—KRIEGE, O. H.: Metall. Trans., *2*, 1971, p. 1627.
[42] CALDERON, H. A.—VOORHEES, P. W.—MURRAY, J. L.—KOSTORZ, G.: Acta Metall., *42*, 1994, p. 991.
[43] ARDELL, A. J.: Interface Sci., *3*, 1995, p. 119.
[44] HIRATA, T.—KIRKWOOD, D. H.: Acta Metall., *25*, 1977, p. 1425.
[45] WHITE, R. J.: Mater Sci. Eng., *33*, 1978, p. 149.